

SOURCE  
DATATRANSPARENT  
PROCESSOPEN  
ACCESS

# Spontaneous development of hepatocellular carcinoma with cancer stem cell properties in PR-SET7-deficient livers

Kostas C Nikolaou<sup>1</sup>, Panagiotis Moulos<sup>1</sup>, George Chalepakis<sup>2</sup>, Pantelis Hatzis<sup>1</sup>, Hisanobu Oda<sup>3,4</sup>, Danny Reinberg<sup>5</sup> & Iannis Talianidis<sup>1,\*</sup>

## Abstract

PR-SET7-mediated histone 4 lysine 20 methylation has been implicated in mitotic condensation, DNA damage response and replication licensing. Here, we show that PR-SET7 function in the liver is pivotal for maintaining genome integrity. Hepatocyte-specific deletion of *PR-SET7* in mouse embryos resulted in G2 phase arrest followed by massive cell death and defect in liver organogenesis. Inactivation at postnatal stages caused cell duplication-dependent hepatocyte necrosis, accompanied by inflammation, fibrosis and compensatory growth induction of neighboring hepatocytes and resident ductal progenitor cells. Prolonged necrotic regenerative cycles coupled with oncogenic STAT3 activation led to the spontaneous development of hepatic tumors composed of cells with cancer stem cell characteristics. These include a capacity to self-renew in culture or in xenografts and the ability to differentiate to phenotypically distinct hepatic cells. Hepatocellular carcinoma in PR-SET7-deficient mice displays a cancer stem cell gene signature specified by the co-expression of ductal progenitor markers and oncofetal genes.

**Keywords** ductal progenitors; hepatocellular carcinoma; histone methylase

**Subject Categories** Cancer; Chromatin, Epigenetics, Genomics & Functional Genomics; Development & Differentiation

**DOI** 10.15252/embj.201489279 | Received 16 June 2014 | Revised 5 November 2014 | Accepted 11 November 2014 | Published online 16 December 2014

**The EMBO Journal (2015) 34: 430–447**

See also: **S Pilz & G Schotta** (February 2015)

## Introduction

Increasing evidence suggests that a relatively rare (1–6%) population of tumor cells—called cancer stem cells (CSC)—with capacities

for self-renewal and differentiation to various cell types is responsible for the maintenance of heterogeneous lineages within tumors (Magee *et al*, 2012). Using various markers, putative cancer stem cells have been identified in many tumor types, including hepatocellular carcinoma (Yang *et al*, 2008; Ma *et al*, 2010; Majumdar *et al*, 2012; Medema, 2013; Zhao *et al*, 2013). Cancer stem cell properties correlate with increased tumor invasiveness and resistance to cytotoxic chemotherapeutics (Magee *et al*, 2012).

The origin of CSCs is poorly understood. In principle, they may arise via de-differentiation or re-programming of terminally committed cells as they traverse the multistep oncogenic transformation process. Recent studies in glioblastomas, breast or intestinal tumors demonstrated that CSCs may indeed derive from the oncogene-induced conversion of mature cells via dysregulation of specific genetic pathways (Friedmann-Morvinski *et al*, 2012; Chaffer *et al*, 2013; Schwitalla *et al*, 2013). Importantly, it was shown that epithelial–mesenchymal transition (EMT) leads to cellular de-differentiation and the generation of cells with stem cell properties (Chaffer *et al*, 2013).

An alternative, less-explored possibility suggests that CSCs may originate from oncogenic transformation of normal adult progenitor cells, which retain self-renewal properties but acquire genetic or epigenetic mutations. In the liver, *bona fide* adult progenitors have recently been characterized using novel markers, including FoxL1, MIC1–1C3, CD133, SOX9 and Lgr5 (Sackett *et al*, 2009; Dorrell *et al*, 2011; Furuyama *et al*, 2011; Shin *et al*, 2011; Huch *et al*, 2013; Miyajima *et al*, 2014). These cells normally reside in biliary ducts and are activated under specific hepatocyte damaging conditions. Persistent liver damage triggers the so-called oval cell response, a regenerative process whereby progenitor cells proliferate and differentiate into hepatocytes or biliary epithelial cells. Notwithstanding, liver regeneration after most forms of acute injury or 2/3<sup>rd</sup> partial hepatectomy does not rely on progenitor cell activation, but instead involves the proliferation of existing previously quiescent hepatocytes (Malato *et al*, 2011; Español-Suñer *et al*, 2012; Schaub *et al*,

1 Biomedical Sciences Research Center Al. Fleming, Vari, Greece

2 Department of Biology University of Crete, Herakleion, Greece

3 Medical Institute of Bioregulation, Kyusyu University, Fukuoka, Japan

4 Gastrointestinal and Oncology Division, National Kyusyu Cancer Center, Fukuoka, Japan

5 HHMI, Department of Biochemistry, New York University School of Medicine, New York, NY, USA,

\*Corresponding author. Tel: +30 210 9653773; E-mail: talianidis@fleming.gr

2014; Yanger *et al*, 2014). Progenitor-dependent regeneration is probably restricted to chronic injury conditions coupled with impaired hepatocyte replication potential (Yamaji *et al*, 2010; Friedman & Kaestner, 2011; Wang *et al*, 2011; Miyajima *et al*, 2014).

Our present study, originally focusing on the role of PR-SET7 in the liver, revealed that hepatocyte-specific *PR-SET7* KO mice represent a useful model for exploring the activation of adult hepatic progenitor cells, since PR-SET7 deficiency leads to cell cycle arrest (Beck *et al*, 2012b). PR-SET7 is the sole enzyme catalyzing histone H4 lysine 20 monomethylation (H4K20Me<sub>1</sub>), a key epigenetic modification that regulates genome integrity in several ways (Beck *et al*, 2012b). H4K20Me<sub>1</sub> is required for DNA repair as it provides a surface for the recruitment of 53BP1 to sites of DNA damage. H4K20Me<sub>1</sub> is a substrate for further methylation to H4K20Me<sub>2</sub> and H4K20Me<sub>3</sub> by Suv4-20h enzymes, which are required for DNA double-strand (DSB) repair (Oda *et al*, 2009, 2010) and facilitate the formation of higher order chromatin structures during mitotic condensation (Oda *et al*, 2009). PR-SET7 protein levels are tightly regulated during the cell cycle via CRL4<sup>Cdt2</sup>-regulated proteolysis (Abbas *et al*, 2010; Centore *et al*, 2010; Oda *et al*, 2010). They are highest in G2/M and early G1 phase and undetectable in S-phase (Oda *et al*, 2009). Interference with this process leads to unscheduled licensing of replication origins and altered timing of mitotic chromosome compaction (Beck *et al*, 2012a). Mouse embryos deficient in PR-SET7 display early lethality due to G2 or M phase arrest associated with chromosomal anomalies and massive cell death prior to the eight-cell stage (Oda *et al*, 2009). This has prevented studies of PR-SET7 function in developing organs. We therefore generated hepatocyte-specific *PR-SET7* knockout mice and investigated the effect of PR-SET7 deficiency in liver organogenesis, hepatocyte proliferation and liver regeneration. Our results demonstrate that in these mice, hepatocyte death initially leads to the activation of ductal progenitors and inflammation, followed by spontaneous development of hepatocellular carcinoma comprised mainly of cells featuring cancer stem cell properties.

## Results

### PR-SET7 deficiency in embryonic hepatocytes impairs liver organogenesis

Mice carrying hepatocyte-specific deletion of *PR-SET7* in embryonic liver were generated by crossing *PR-SET7<sup>loxP</sup>* mice (Oda *et al*, 2009) with *Alfp-Cre* mice. Complete inactivation of *PR-SET7* in hepatocytes was observed as early as embryonic day 15.5 (E15.5) in homozygous *PR-SET7<sup>loxP</sup>/Alfp-Cre* (designated *PR-SET7<sup>ΔHepE</sup>*, i.e. Embryonic-Hepatocyte Deletion) mice. None of these mice reached birth. Live embryos at E18.5 had anemic appearance and dramatically reduced liver size, while other organs looked normal (Fig 1A). Hematoxylin and eosin and immunostaining for albumin revealed a dramatic reduction of hepatocytes in *PR-SET7<sup>ΔHepE</sup>* embryonic liver strips (Fig 1B and C). We also detected decreased mRNA levels of hepatocyte-specific marker genes (Fig 1D). The few residual hepatocyte-like cells had a more eosinophilic appearance and enlarged nuclei with sponge-like condensation of chromatin (Fig 1B), reminiscent of cells in G2/M phase or of necrotic cells. Arrest in G2 phase of the cell cycle was confirmed by positive staining with cyclin B1

antibody (Fig 1E). Strong staining for  $\gamma$ H2AX was indicative of extensive DNA damage (Fig 1F). These results suggest that PR-SET7 is required for normal hepatocyte growth and liver organogenesis during embryonic life.

### Cell division-dependent DNA damage, necrosis and altered H4K20 methylation patterns in PR-SET7-deficient adult hepatocytes

To inactivate PR-SET7 in postnatal hepatocytes, we crossed *PR-SET7<sup>loxP</sup>* mice with *Alb-Cre* mice. Complete loss of PR-SET7 in the hepatocytes of these mice (designated *PR-SET7<sup>ΔHepA</sup>*, i.e. Adult-Hepatocyte Deletion) was observed as early as postnatal day 20 (P20) (Supplementary Fig S1A). Examination of the livers 25 days later (at P45) revealed no visible morphological or histological changes (Supplementary Fig S1B and C). Interestingly, global H4K20 monomethylation was not affected (Supplementary Fig S1D), although PR-SET7 was clearly absent from all hepatocytes (Supplementary Fig S1E). Importantly, loss of PR-SET7 was observed only in hepatocytes and not in biliary epithelial cells (Supplementary Fig S1E). In the adult liver, most hepatocytes are in the G0 phase of the cell cycle. Since the median number of cell duplications in the liver between P20 (when *PR-SET7* is deleted in our model) and P45 is less than one (Supplementary Fig S2A), the above finding suggests that H4K20Me<sub>1</sub> is a relatively stable modification, which is preserved in non-dividing cells, even in the absence of PR-SET7.

At 4 months (P120), small regenerative foci became visible in *PR-SET7<sup>ΔHepA</sup>* livers (Fig 2A). By this age, a significant number of cells that existed in P20 are expected to have gone through at least one cell duplication. Hematoxylin and eosin staining of liver sections from P120 *PR-SET7<sup>ΔHepA</sup>* mice revealed three morphologically distinct areas: one with normal hepatocyte appearance (Area-A), probably corresponding to cells that have not yet divided; a second, containing enlarged hepatocytes infiltrated with small mononuclear cells (Area-B; named Necrotic Zone); and a third, containing smaller sized parenchymal cells, resembling hepatocytes in regenerating liver (Area-C; named Regenerative Zone, see below) (Fig 2B). All of the large cells in Area-B and the smaller cells in Area-C were HNF4-positive hepatocytes (Fig 2C).

Accumulation of apoptotic cells in the 'Necrotic Zone' could be detected by TUNEL staining (Fig 2D). These cells, however, correspond to infiltrating non-hepatic cell types, since the enlarged hepatocytes were always TUNEL negative (Fig 2D). On the other hand, all of the large hepatocytes stained positively for  $\gamma$ H2AX, 53BP1 and cyclin B1, demonstrating that these cells have suffered massive DNA damage and were arrested in the G2 phase (Fig 2E, Supplementary Fig S2B and C). In agreement with the lack of TUNEL staining, the electron microscopic profile of the large cells lacked the characteristic hallmarks of apoptosis (e.g. nuclear condensation, membrane blebbing) (Fig 3A). On the other hand, the large cells had all the known morphological characteristics of necrosis that distinguish them from apoptotic cells. These include increased cell volume that does not fragment into discrete corpses, disrupted cellular membrane, translucent cytoplasm, swollen mitochondria and disorganized endoplasmic reticulum (Fig 3A).

Examination of the nuclear H4K20Me<sub>1</sub> staining profile at the different areas of P120 *PR-SET7<sup>ΔHepA</sup>* livers revealed unchanged patterns in normal hepatocytes (in Area-A) but a complete loss of

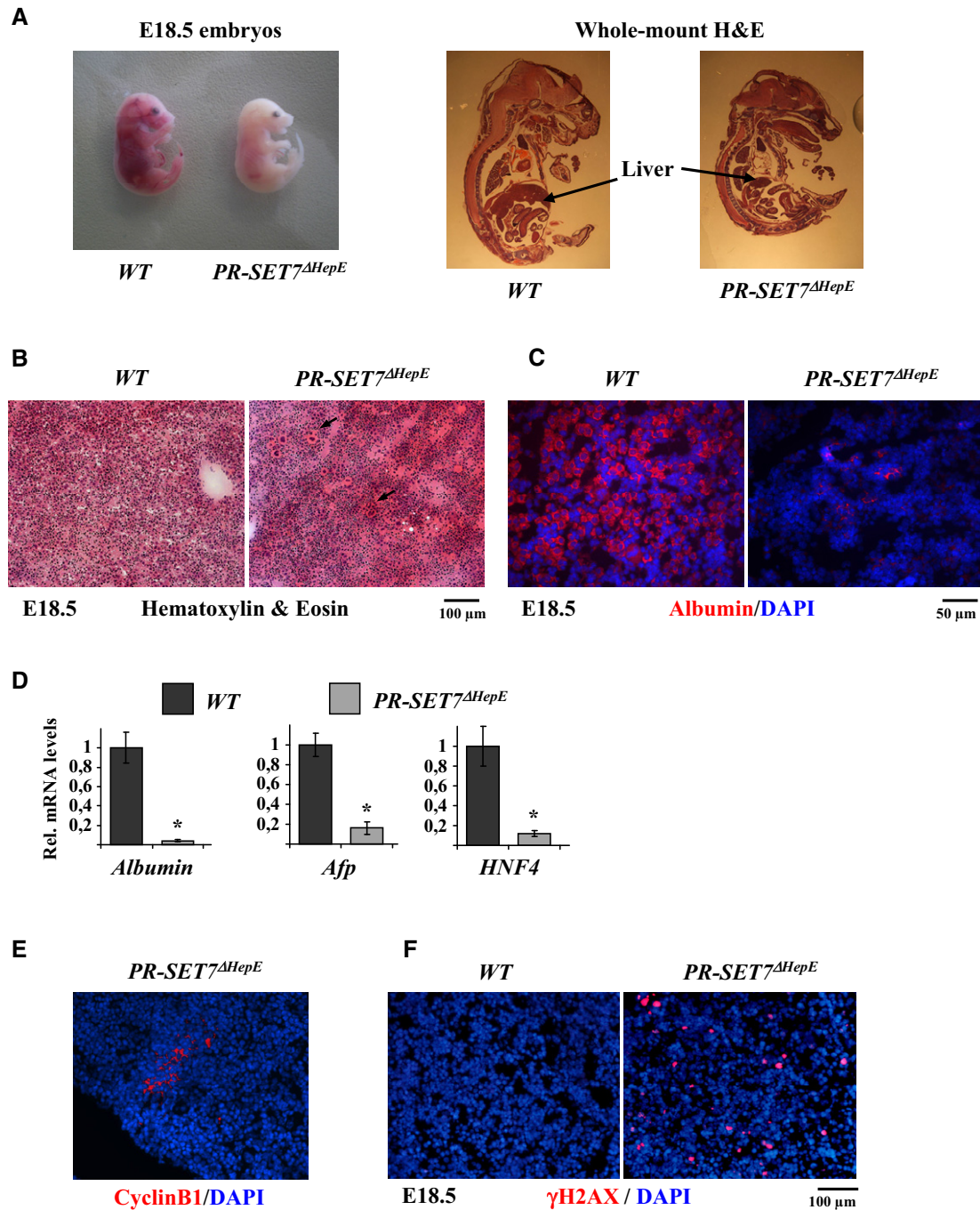


**Figure 1. PR-SET7 is required for proper liver organogenesis during embryonic development.**

A Representative pictures of embryos at 18.5 days postcoitum (E18.5) and hematoxylin and eosin staining of whole-mount embryo sections from *PR-SET7<sup>loxP</sup>/Alfp-Cre* (*PR-SET7<sup>ΔHepE</sup>*) mice and control littermates (*WT*).

B Hematoxylin and eosin staining of liver sections.

C Immunohistochemical staining of liver sections with albumin antibody.

D qPCR analysis of *Albumin*, *Afp* and *HNF4* mRNA levels. Bars represent mean values of mRNA levels normalized to glyceraldehyde-3-phosphate dehydrogenase (*GAPDH*) mRNA and SEM from samples of four individual mice. \**P*-value < 0.01.

E Immunohistochemical staining of liver sections with cyclin B1 antibody.

F Immunohistochemical staining of liver sections with  $\gamma$ H2AX antibody.

H4K20Me<sub>1</sub> immunoreactivity in the nuclei of the large necrotic hepatocytes (in Area-B; Fig 3B). Since PR-SET7 is the sole enzyme capable of generating H4K20Me<sub>1</sub>, this suggests that the H4K20Me<sub>1</sub>

mark is highly stable in non-dividing cells, as it can persist for at least 100 days in the complete absence of the enzyme. The disappearance of H4K20Me<sub>1</sub> staining in the large necrotic

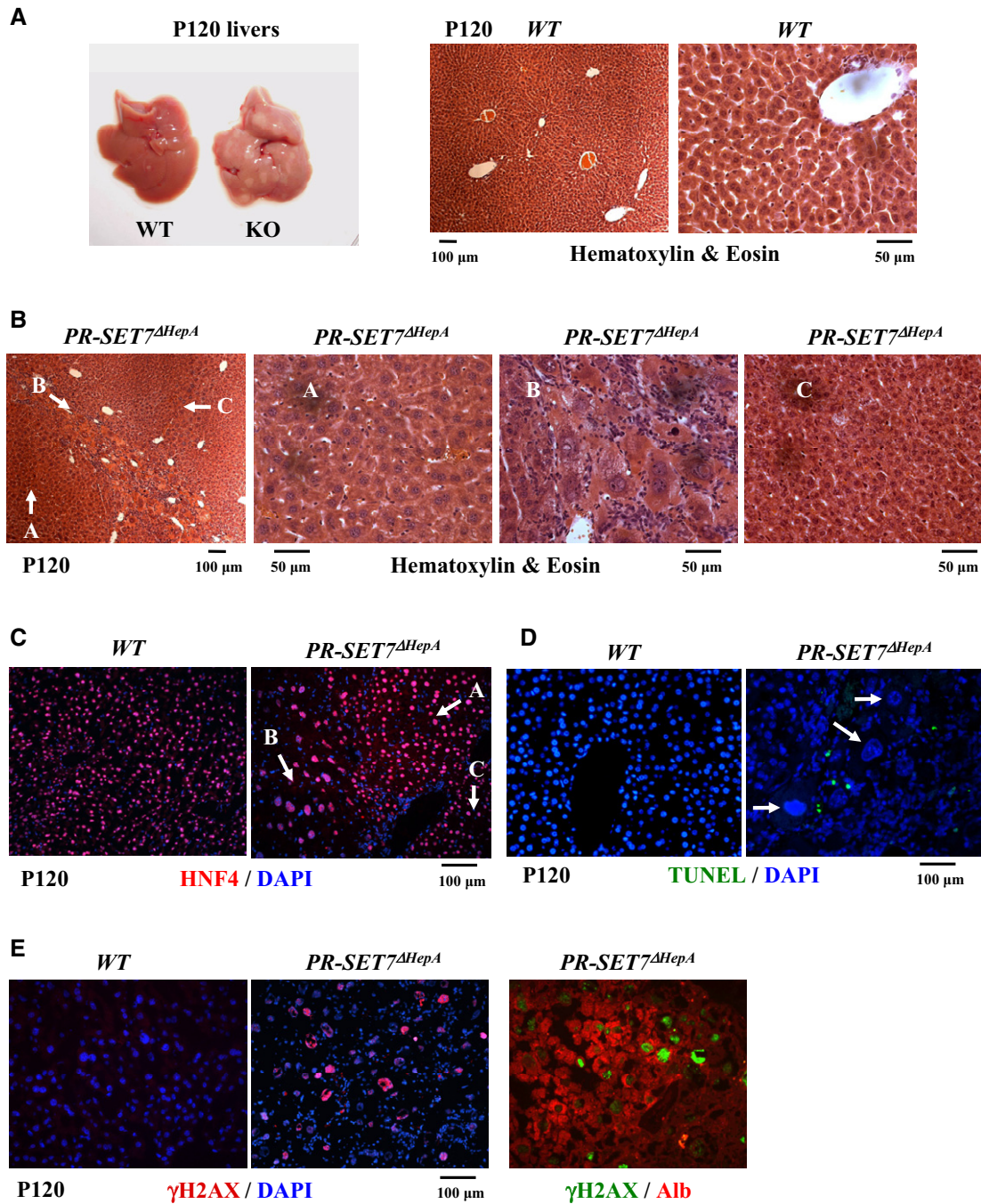


**Figure 2.** Postnatal inactivation of PR-SET7 in hepatocytes leads to cell death.

A Macroscopic appearance of livers in 120-day-old (P120) wild-type (WT) and *PR-SET7<sup>loxP</sup>/Alb-Cre* (KO) mice. Note, small adenomatous foci in KO livers.

B Representative hematoxylin and eosin staining of liver sections from P120 wild-type (WT) and *PR-SET7<sup>loxP</sup>/Alb-Cre* (*PR-SET7<sup>ΔHepA</sup>*) mice. Arrows show three areas containing morphologically different hepatocytes. Right panels: zoom-in to Area-A—'normal zone', to Area-B—'necrotic zone' and to Area-C—'regenerative zone'.

C Immunohistological staining of liver sections from P120 *PR-SET7<sup>ΔHepA</sup>* mice and control littermates (WT) with HNF4 antibody.

D TUNEL staining of liver sections from P120 *PR-SET7<sup>ΔHepA</sup>* mice and control littermates (WT). Note that cells containing enlarged nuclei (white arrows) are TUNEL negative.

E Immunohistological staining with γH2AX and albumin (Alb) antibodies.

hepatocytes could be explained by assuming that these cells represent a population of hepatocytes that have undergone several cell divisions. However, PR-SET7-deficient cells are not able to

progress beyond 1.5 cell divisions, as they are arrested in the G2 phase of the next cell cycle (Oda *et al.*, 2009; Supplementary Fig S2C). Thus, following inactivation, the staining signal is

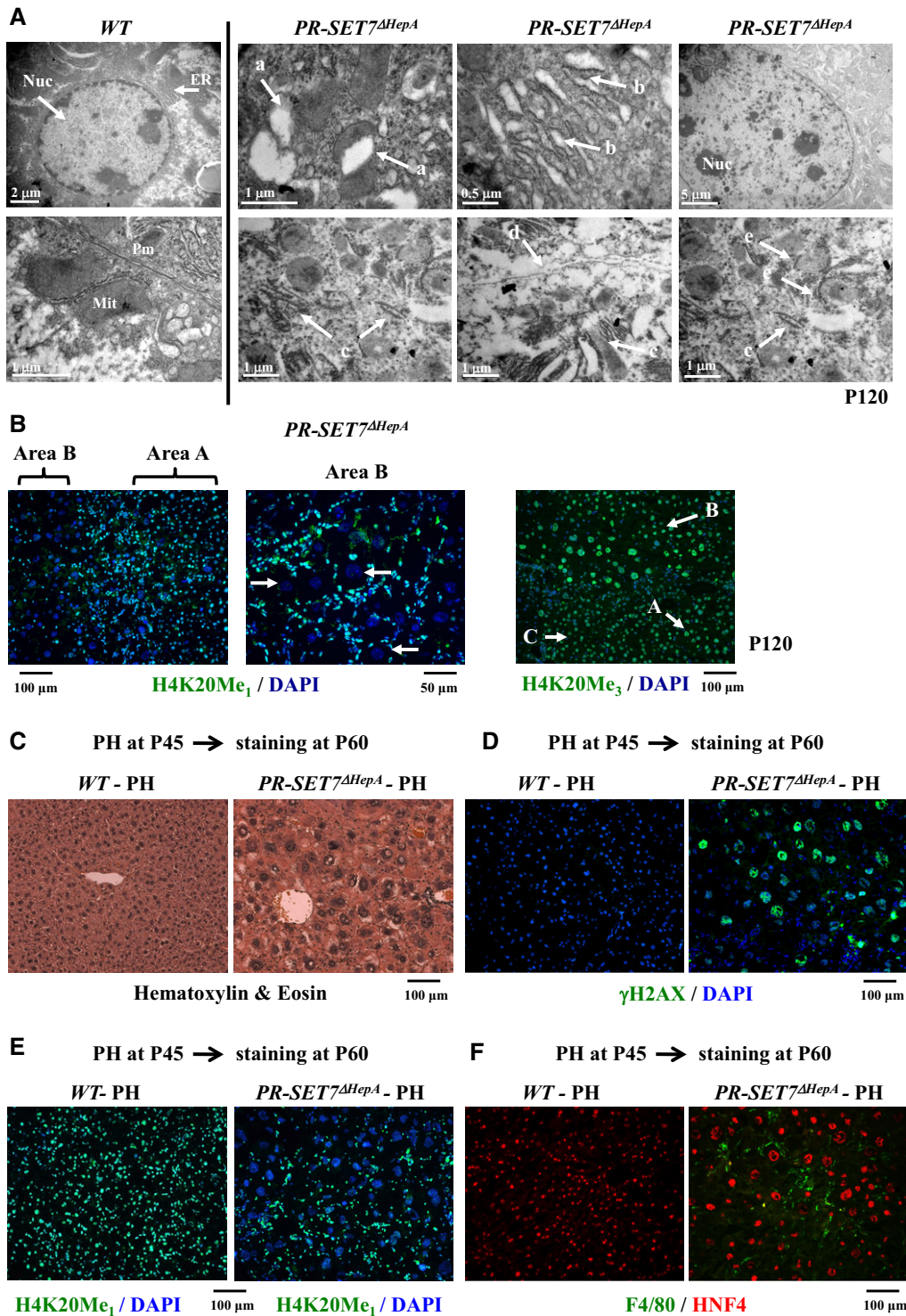


**Figure 3. PR-SET7-deficient hepatocytes die via necrosis in a cell division-dependent manner.**

**A** Electronmicroscopic images of cells containing enlarged nuclei in P120 *PR-SET7<sup>ΔHepA</sup>* livers and normal hepatocytes in control littermates (WT). White arrows indicate: (Nuc) nuclei; (ER) endoplasmic reticulum; (Mit) mitochondrium; (PM) plasma membrane; (a) swollen mitochondria; (b) swollen endoplasmic reticulum; (c) disorganized endoplasmic reticulum; (d) disrupted plasma membrane; and (e) disorganized pieces of endoplasmic reticulum encircling mitochondria to form autophagosomes.

**B** Immunohistochemical staining of liver sections from P120 *PR-SET7<sup>ΔHepA</sup>* mice and control littermates (WT) with H4K20Me<sub>1</sub> and H4K20Me<sub>3</sub> antibodies. Normal (Area-A), Necrotic (Area-B) and Regenerative (Area-C) hepatocyte-containing areas are indicated. Arrows show the loss of H4K20Me<sub>1</sub> signal from the large necrotic nuclei.

**C–F** Partial (2/3<sup>rd</sup>) hepatectomy was performed in 45-day-old *PR-SET7<sup>ΔHepA</sup>* mice and control littermates (WT). Two weeks later, at postnatal day 60 (P60) liver sections were stained with hematoxylin and eosin (C) or γH2AX (D) or H4K20Me<sub>1</sub> (E) or HNF4 and F4/80 (F) antibodies.

expected to decrease to half, at most. The observed complete loss of the H4K20Me<sub>1</sub> signal is most likely the result of its 'up-methylation' to the H4K20Me<sub>3</sub> form in G2/M arrested cells. This latter scenario is supported by the detection of H4K20 trimethylation in the enlarged, necrotic hepatocytes (Fig 3B).

The abovementioned morphological alterations combined with the H4K20Me<sub>1</sub> staining pattern provided an initial indication that PR-SET7 deficiency has little effect in non-dividing cells, but induces cell cycle arrest, extensive DNA damage and necrosis only in dividing cells. To provide direct evidence for this scenario, we performed 2/3<sup>rd</sup> partial hepatectomy, an experimental setup in which quiescent G0-phase hepatocytes synchronously enter the cell cycle and undergo an average of 1.5 cell divisions. Partial hepatectomy was performed at P45, when PR-SET7 was completely absent from hepatocytes for at least 25 days (Supplementary Fig S1E). Two weeks later, the original liver mass had recovered in both wild-type and PR-SET7<sup>ΔHepA</sup> mice, but all of the hepatocytes in regenerated PR-SET7<sup>ΔHepA</sup> livers were enlarged, stained positively for γH2AX and HNF4, had lost nuclear H4K20Me<sub>1</sub> and retained H4K20Me<sub>3</sub> immunoreactivity (Fig 3C–E, Supplementary Fig S2D and E).

Taken together, the above results suggest that in the absence of PR-SET7, dividing hepatocytes are cell cycle arrested and undergo necrotic death. This leads to the essentially complete elimination of all PR-SET7-deficient hepatocytes in conditions when hepatocytes are rapidly dividing (e.g. embryonic liver and in adults after partial hepatectomy).

#### Induction of regenerative processes to compensate for liver damage in PR-SET7<sup>ΔHepA</sup> mice

In P120 PR-SET7<sup>ΔHepA</sup> livers, Ki67 staining detected proliferating cells in areas B and C. None of the large cells in Area-B stained positively for Ki67 (Fig 4A). Proliferating hepatocytes (Ki67/albumin double-positive cells) were detected only in Area-C, while all Ki67-positive cells in Area-B lacked Alb staining (Fig 4A). These results indicate that in Area-B, the enlarged necrotic hepatocytes are infiltrated by other proliferating cells types (e.g. inflammatory cells or ductal cells), while Area-C (Regenerative Zone) contains hepatocytes that have entered the cell cycle to compensate for the dying cells.

Immunostaining with the 'oval cell' marker A6 revealed a parallel expansion of adult hepatic progenitor cells in the 'Necrotic Zone', which started to migrate into the 'Regenerative Zone' (Fig 4B). Importantly, these proliferating oval cells at P120 did not express the hepatic marker HNF4 (Fig 4B). The initial activation and migration of adult ductal progenitor cells, which have not yet differentiated to hepatocytes, were confirmed by staining with another progenitor cell marker Sox9 (Supplementary Fig S2F). Activation of hepatic ductal progenitors requires FGF7 functional niche signal (Takase *et al*, 2013). In line with this, we detected excessive amounts of FGF7 protein in the vicinity of the A6-positive cells and a dramatic increase of FGF7 mRNA in P120 PR-SET7<sup>ΔHepA</sup> livers (Fig 4C and D).

Collectively, the data suggest that hepatocyte death in PR-SET7-deficient hepatocytes triggers two types of regenerative processes: proliferation of neighboring hepatocytes, which, due to the absence of PR-SET7, are destined to die, and the proliferation of ductal progenitors, which are induced by a cellular microenvironment producing FGF7. Consistent with this, in P120 PR-SET7<sup>ΔHepA</sup> livers,

we could detect non-parenchymal cells staining positively for PR-SET7 (Supplementary Fig S1F).

#### Hepatocyte necrosis in PR-SET7<sup>ΔHepA</sup> mice triggers extensive inflammation, fibrosis, ROS accumulation and the activation of STAT3 in the liver

The smaller sized mononuclear cells accumulating in the 'Necrotic Zone' of P120 or regenerating P60 PR-SET7<sup>ΔHepA</sup> livers were identified as inflammatory cells by immunostaining with the F4/80 macrophage marker and the CD45 pan-leukocyte markers (Supplementary Fig S3A and B, Fig 3F). These cells expressed PR-SET7 and always stained positively for H4K20 methylation (Supplementary Fig S1F, Fig 3B). Cell death-associated inflammation was accompanied by extensive fibrosis as evidenced by Sirius Red staining (Supplementary Fig S3C) and the production of pro-inflammatory cytokines TNF-α and IL-6 (Supplementary Fig S3D and E). While significant increases in TNF-α and IL-6 expression were evident at 120-day-old PR-SET7<sup>ΔHepA</sup> livers, maximal inductions were detected 4 months later in P240 livers (Supplementary Fig S3D and E). A similar temporal increase in reactive oxygen species (ROS) accumulation was detected by staining the liver sections with the H<sub>2</sub>O<sub>2</sub>-sensitive fluorescent dye CM-H<sub>2</sub>DCFDA (Fig 5A). IL-6 and ROS accumulation is expected to induce the activation of the oncogenic transcription factor STAT3 (He & Karin 2011; Nikolaou *et al*, 2012). Indeed, strong activation of STAT3 was detected in P240 PR-SET7<sup>ΔHepA</sup> livers by immunostaining and by Western blot analysis using a phospho-STAT3 antibody (Fig 5B and C).

#### Late-onset, spontaneous development of hepatocellular carcinoma in PR-SET7<sup>ΔHepA</sup> mice

P240 PR-SET7<sup>ΔHepA</sup> mice had elevated serum ALT levels, and their livers contained numerous visible cancerous nodules of different sizes (Fig 5D and E). The penetrance of liver cancer was 100% as judged by the examination of more than 40 mice at ages 240–300 days. Microscopic evaluation revealed several histopathological features of hepatocellular carcinoma, including irregular trabeculae, obliteration of portal tracts, frequent pleomorphism, nuclear atypia and cells with increased eosinophilic inclusions or cytoplasmic clearance (Fig 5F). The development of a full-blown hepatocellular carcinoma in P240 PR-SET7<sup>ΔHepA</sup> mice was further confirmed by the increased mRNA levels of oncofetal marker genes *Afp*, *H19*, *GPC3* and *CTGF* (Fig 5G), the positive staining of hepatocytes by *Afp* (Fig 6A) and the Ki-67 proliferation marker (Fig 6B). We further investigated 12 microdissected tumors and age-matched wild-type livers by array-based comparative genomic hybridization (CGH) for chromosomal aberrations. A large number of amplifications and deletions were detected in most chromosomes ranging from 12 kB to 1.58 MB (Supplementary Fig S4). The pattern of the aberrations varied in samples from different animals and also from two different HCC foci in the same liver. Some of the abnormalities, however, were present in all 12 HCC foci examined, which may correspond to common genomic hotspots highly susceptible to deletions or amplifications.

Since PR-SET7 deficiency causes G2 phase arrest and necrotic cell death, the expansion of highly proliferating cancerous hepatocytes in P240 PR-SET7<sup>ΔHepA</sup> livers can only be explained by the

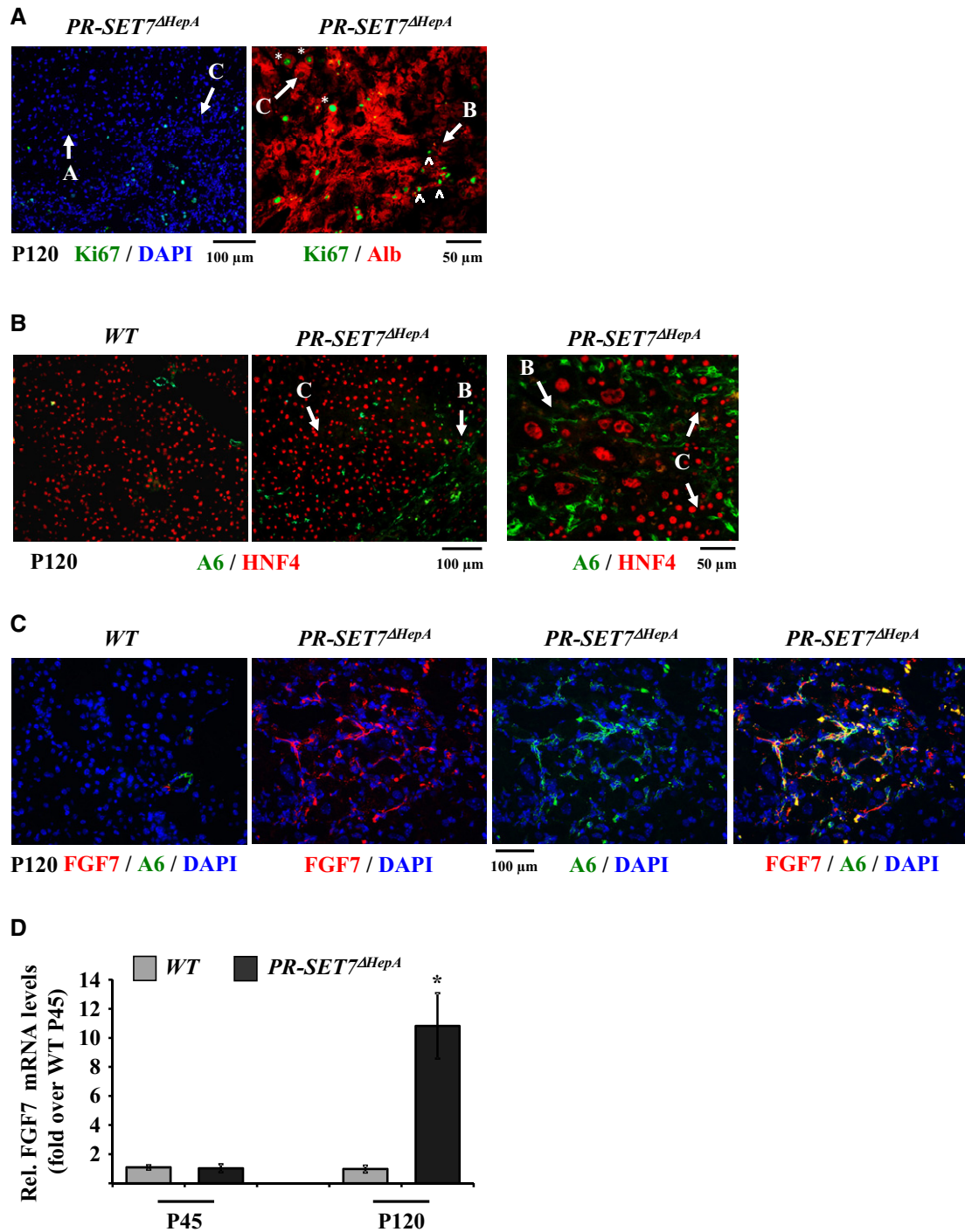


**Figure 4. Compensatory proliferation of neighboring hepatocytes and ductal progenitor cells in FGF7 signal-containing microenvironment.**

A, B Immunohistological staining of liver sections from P120 *PR-SET7<sup>ΔHepA</sup>* mice and control littermates (WT) with Ki67, albumin (Alb) and A6 or HNF4 antibodies as indicated. Arrows depict the different areas in the sections as indicated above (Fig. 1B). Asterisks (\*) indicate Ki67<sup>+</sup> hepatocytes. Small arrows (-) indicate Ki67<sup>+</sup> non-hepatic cells. Note the lack of co-staining of cells with HNF4 and A6 antibodies.

C Immunohistological staining of liver sections from P120 *PR-SET7<sup>ΔHepA</sup>* mice and control littermates (WT) with FGF7 and A6 antibodies.

D Relative mRNA levels of *FGF7*. Bars represent mean *FGF7* mRNA levels normalized to *GAPDH* mRNA and SEM from samples of 5 individual 45 days or 120-day-old mice. The data are presented as fold over values obtained with wild-type P45 samples. \**P*-value < 0.01.

proliferation of other cell types containing intact *PR-SET7* alleles, which can differentiate to hepatocytes and undergo oncogenic transformation. In agreement with this scenario, in P240 livers we

detected a large number of Ki-67<sup>+</sup> parenchymal cells. Importantly, all of the parenchymal cells expressed the hepatic markers HNF4 and albumin and stained positively for H4K20Me<sub>1</sub> or PR-SET7

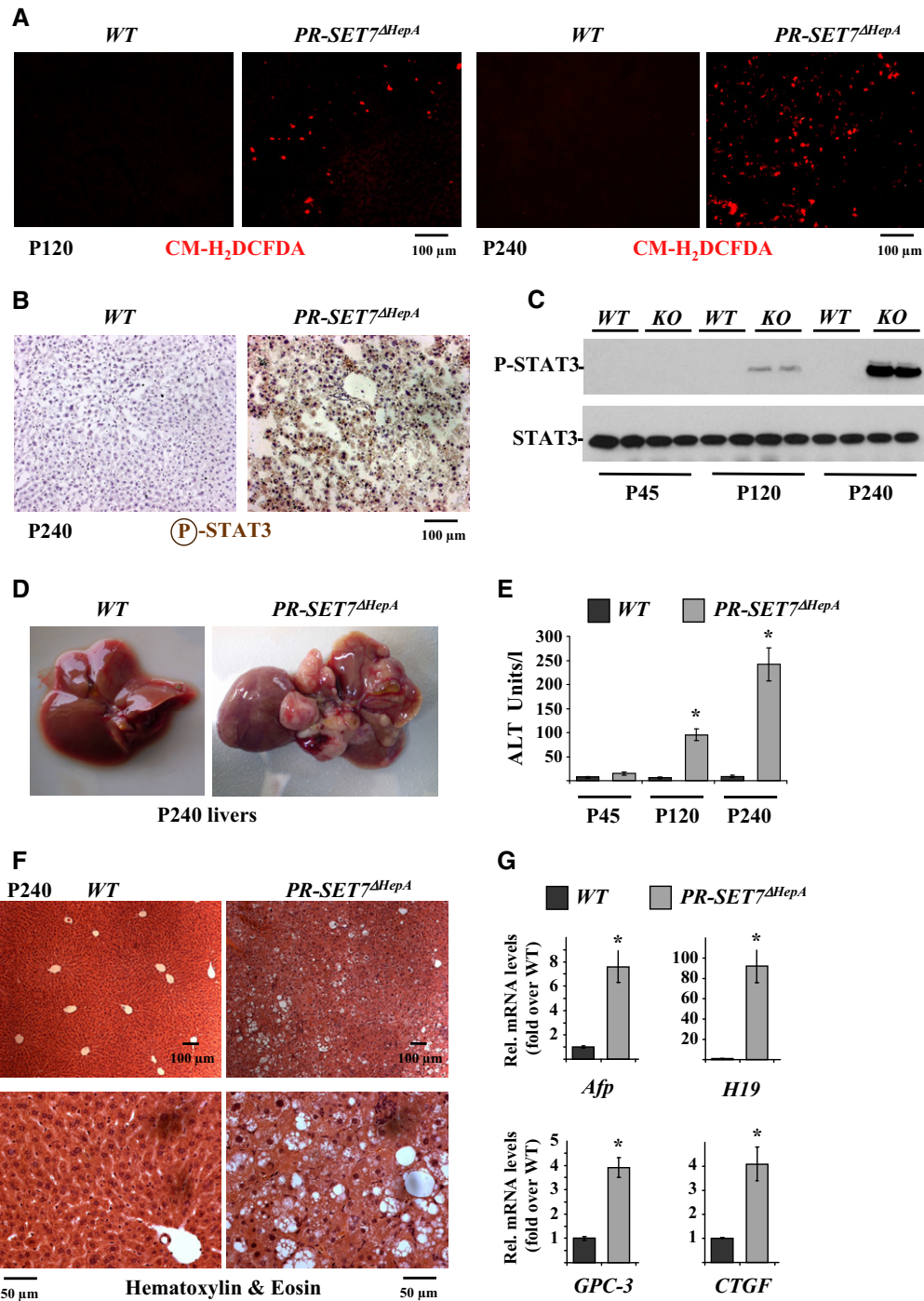


**Figure 5.** ROS accumulation, STAT3 activation and late-onset spontaneous development of hepatocellular carcinoma in *PR-SET7<sup>ΔHepA</sup>* mice.

A Analysis of reactive oxygen species (ROS) accumulation in frozen liver sections from 120-day-old (P120) and 240-day-old (P240) *PR-SET7<sup>ΔHepA</sup>* mice and control littermates (WT).

B Immunohistological staining of liver sections from P240 animals with phospho-STAT3 antibody.

C Western blot analysis of liver extracts from P45, P120 and P240 mice with STAT3 and phospho-STAT3 antibodies.

D Macroscopic appearance of livers in P240 *PR-SET7<sup>ΔHepA</sup>* mice and control littermates (WT).

E Serum alanine aminotransferase (ALT) levels in P45, P120 and P240 mice. Bars represent mean values of ALT levels and SEM from liver extracts of five individual mice. \**P*-value < 0.01.

F Representative hematoxylin and eosin staining of liver sections from P240 *PR-SET7<sup>ΔHepA</sup>* mice and control littermates (WT). Two different magnifications are shown.

G Relative mRNA levels of selected oncofetal genes. Bars represent mean *Afp*, *H19*, *GPC-3* and *CTGF* mRNA levels normalized to *GAPDH* mRNA and SEM from samples of 5 individual 240-day-old mice. The data are presented as fold over values obtained with wild-type samples. \**P*-value < 0.01.

Source data are available online for this figure.

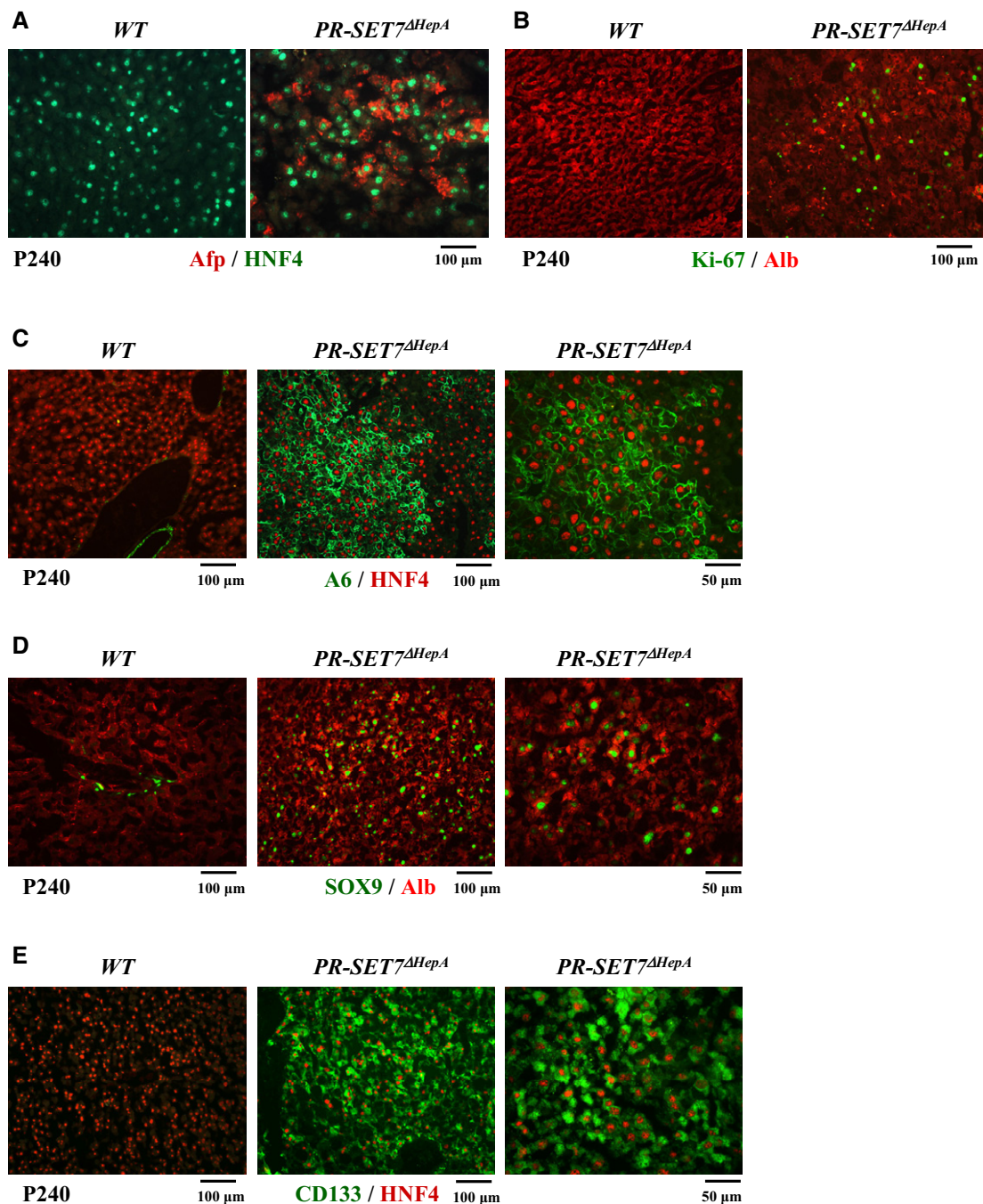


**Figure 6. Hepatocellular carcinoma in P240 PR-SET7-deficient mice is composed of cells expressing hepatic progenitor cell markers.**

A, B Immunohistological staining of liver sections from P240 *PR-SET7<sup>ΔHepA</sup>* mice and control littermates (WT) with Afp and HNF4 (A) or Ki-67 and albumin (Alb) (B) antibodies.

C–E Double staining of liver sections with A6 and HNF4 (C) or Sox9 and Alb (D) or CD133 and HNF4 (E) antibodies. Right panels show larger magnifications of stainings performed in *PR-SET7<sup>ΔHepA</sup>* liver sections.

(Fig 6C–E, Supplementary Fig S5A and B). Taking into the account the fact that PR-SET7 was not detectable in P45 or P120 hepatocytes (Supplementary Fig S1E and F), the above finding suggests that, parallel to the complete elimination of ‘old’ hepatocytes containing inactivated *PR-SET7* alleles, ‘new’ hepatocytes with an intact *PR-SET7* gene arose and repopulated the liver. These hepatocytes may

originate from differentiating resident ductal progenitor cells, as suggested by the co-staining with three different markers, A6, Sox9 and CD133 (Fig 6C–E). They represent a proliferating Ki-67-positive hepatocyte population with a normal H4K20Me<sub>1</sub> staining pattern (Supplementary Fig S5C and D). Since the A6 antibody apart from ‘oval cells’ also marks cholangiocytes (Engelhardt *et al*, 1993; and

Fig 6C wild-type panel), we examined whether part of the A6 positive cells correspond to cholangiocarcinoma cells, which often accumulate in HCC models (Bettermann *et al*, 2010; Nikolaou *et al*, 2012). Staining for the cholangiocyte marker cytokeratin-19 (CK19) revealed that CK19-positive cholangiocytes had not expanded in P240 *PR-SET7<sup>AHepA</sup>* livers (Supplementary Fig S5E). In line with this, the vast majority of A6-positive cells were co-stained with the hepatocyte marker HNF4 (Fig 6C).

In different sections examined, most, but not all, of the ‘new’ hepatocytes stained positively for the individual ductal markers (Fig 6C–E), suggesting that they are derived from a heterogeneous population of cells. In agreement with this, double staining with A6 and Sox9 or CD133 and Sox9 antibodies revealed different percentages of single- and double-positive cells (Fig 7A). Importantly, however, 97 to 99% of the parenchymal cells stained positively with either A6 or Sox9 or CD133 or combinations of them, and only 1–3% scored as double negative. This latter value is below the limits of experimental error in histological assays, which may arise from different local thickness of sections or uneven distribution of the antibodies. Taken together, we conclude that essentially all cancerous hepatocytes in P240 *PR-SET7<sup>AHepA</sup>* livers express PR-SET7 and ductal progenitor markers.

#### Hepatocellular carcinoma in *PR-SET7<sup>AHepA</sup>* mice exhibits cancer stem cell properties

The expression of CD133 and CD44 markers in P240 *PR-SET7<sup>AHepA</sup>* hepatocytes raised the possibility that they correspond to self-renewing cancer stem cells. To provide formal evidence for this, we isolated primary hepatocytes from P240 *PR-SET7<sup>AHepA</sup>* livers and cultured them *in vitro*. The cells survived several passages in culture without any significant reduction of proliferation capacity (Fig 7B) and gave rise to tumors after grafting to immunodeficient mice (Fig 7C). Primary *PR-SET7<sup>AHepA</sup>* hepatocytes generated skin xenograft tumors with efficiency comparable to those generated by the highly tumorigenic hepatic cell line Hepa 1–6 (Fig 7C). Further analysis of the tumor xenografts prepared 20 days after injection revealed that they are composed mainly of A6/HNF4 double-positive cells (Fig 7D), which is characteristic of the parent tumor. The majority (85–90%) of the cells were co-stained with Sox9 and CD133, pointing to the clonal dominance of the A6/Sox9/CD133 positive cell population (Fig 7D). The percentage of A6/HNF4 and CD133/HNF4 double-positive cells decreased in 30-day grafts, while in parallel, an increase of the more differentiated HNF4 single-positive hepatocyte population was detected (Fig 7E). Moreover, duct-like structures, containing A6 single-positive cells were often seen in 30-day grafts (Fig 7E second panel from left). These results demonstrate that the majority of the hepatocytes in P240 *PR-SET7<sup>AHepA</sup>* livers are self-renewing cancer stem cells, which can give rise to phenotypically distinct, less or more differentiated cell types.

Gene expression profiling by RNA sequencing revealed 1,415 differentially expressed genes (527 genes downregulated and 888 genes upregulated) in P240 *PR-SET7<sup>AHepA</sup>* livers compared to wild-type ones (Fig 8A). The ‘upregulated’ gene set contained progenitor markers (Sox9, CD44, Prom1/CD133, Dlk1, Sox4), hepatic oncofetal markers (H19, Igf2, Gas5, Akr1b7, Afp, Igfbp1, Hn1) and proliferation markers (Cnd1, Ccne1), while the ‘downregulated’ gene set was enriched in genes expressed specifically in terminally

differentiated hepatocytes (Mup3, Tat, Cyp7A1, Gck, Acsl1, ApoA5 and others) (Fig 8B). This pattern suggests that hepatic cancer stem cells can be characterized by a specific gene expression signature, which is supported by the comparison with the differentially expressed genes in ductal progenitor cells (Lgr5-LacZ<sup>+</sup> and MIC1C3) isolated from non-cancerous livers (Huch *et al*, 2013). Lgr5-LacZ<sup>+</sup> and MIC1C3 represent different ductal progenitor populations as suggested by the high, but not complete, overlap (37% in the ‘upregulated’ and 63% in the ‘downregulated’ gene set) of the differentially expressed genes (Fig 8C and D, Supplementary Fig S6B–D). About 35% of differentially expressed genes in P240 *PR-SET7<sup>AHepA</sup>* livers (34.9% in the ‘upregulated’ and 35.7% in the ‘downregulated’ gene set) were also expressed differentially in the same direction in either Lgr5-LacZ<sup>+</sup> or MIC1C3 cells or both. The overlap between the differentially expressed genes was statistically highly significant ( $P < 10^{-5}$ ), pointing to a biological relationship. Inspection of genes that are upregulated in all three sources (93 genes) revealed the presence of known progenitor markers such as Sox9, CD44 or Itga6, while genes that are upregulated only in P240 *PR-SET7<sup>AHepA</sup>* livers contained hepatic oncofetal genes such as Afp, H19 or Igfbp1 (Fig 8C). In the commonly downregulated category, marker genes for terminally differentiated hepatocytes, such as Tat, Gck or Cyp7A1 were identified. Finally, the set of genes that were downregulated only in P240 *PR-SET7<sup>AHepA</sup>* livers contained several tumor suppressors such as Irf2, Gas1, Eaf2 or Cited2 (Fig 8D).

The genes differentially expressed between the recently described HCC progenitor cells (HcPC) (He *et al*, 2013) and wild-type livers also exhibited an overlap with those detected in Lgr5-LacZ<sup>+</sup> or MIC1C3 (40.6% in the upregulated gene set and 32.9% in the downregulated gene set) (Supplementary Fig S6B). These values are similar to those detected in comparisons of P240 *PR-SET7<sup>AHepA</sup>* livers and Lgr5-LacZ<sup>+</sup> or MIC1C3. However, direct comparison of the P240 *PR-SET7<sup>AHepA</sup>* and HcPC transcriptomes revealed significantly smaller numbers of common genes (7.5% of upregulated and 3.8% of downregulated genes Supplementary Fig S6A and B), suggesting that HcPCs and the P240 *PR-SET7<sup>AHepA</sup>* carcinoma cells correspond to distinct cell populations.

We have also determined the gene expression profile of diethylnitrosamine (DEN) treatment-induced hepatic tumors, which originate from compensatory proliferation of existing hepatocytes (Kang *et al*, 2007; He & Karin, 2011). In these tumors, A6- and Sox9-positive cells do exist, but their proportion is very low, corresponding to about 2–5% of the hepatocyte population (Supplementary Fig S7A). As expected, a large number of differentially expressed genes were common in P240 *PR-SET7<sup>AHepA</sup>* liver tumors and DEN treatment-generated tumors, as both display primarily HCC features. The correlation value ( $\rho = 0.713$ ), however, illustrates that substantial differences also exist: The detection of a large number of differentially expressed genes in either the same or the opposite direction suggests that these tumors also have unique characteristics, which distinguish them from each other (Supplementary Fig S7B). Importantly, the expression of most progenitor marker genes was significantly increased in P240 *PR-SET7<sup>AHepA</sup>* liver tumors (Supplementary Fig S7B).

Taken together, the above findings suggest that P240 *PR-SET7<sup>AHepA</sup>* livers are repopulated by cells expressing ductal and cancer stem cell markers, which possess self-renewing capacity and generate xenografts that are representative of the parent tumor. Furthermore,

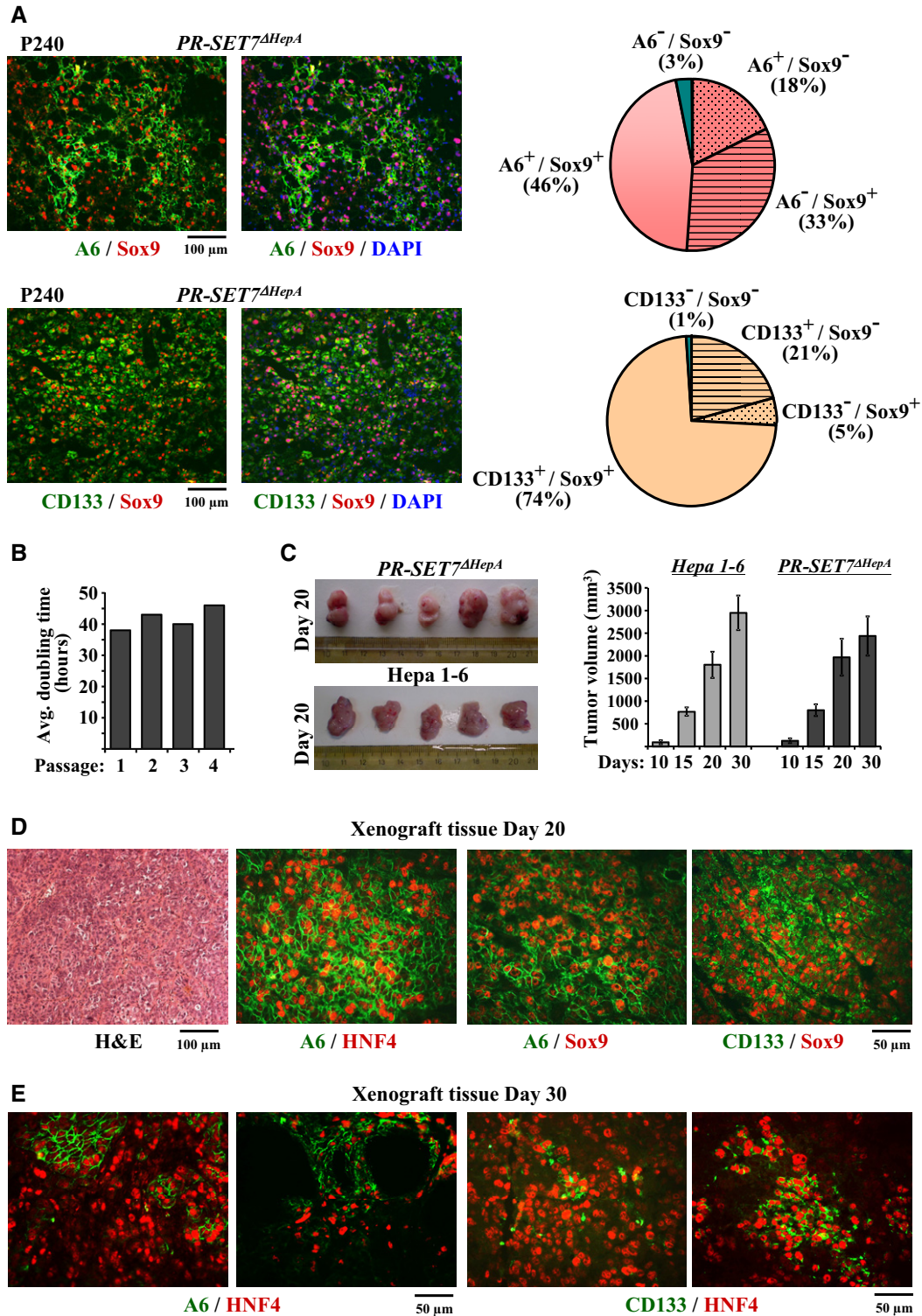


**Figure 7. Quantitative assessment and xenograft tumor formation potential of progenitor-derived carcinoma cells.**

- A P240 *PR-SET7<sup>ΔHepA</sup>* liver sections were double-stained with A6 and Sox9 (upper panel) or CD133 and Sox9 (lower panel). Pie charts at the right represent average percentages of cells stained positively with the indicated markers after counting DAPI-stained cells in 5 high-power fields (HPF) in liver sections of 3 different mice.
- B Cell duplication rate of primary hepatocytes from P240 *PR-SET7<sup>ΔHepA</sup>* livers in culture.
- C Pictures of representative subcutaneous xenograft tumors dissected from immunodeficient mice 20 days after injection with primary hepatocytes from P240 *PR-SET7<sup>ΔHepA</sup>* livers or Hepa 1–6 cells. Right panel shows average tumor volumes ( $n = 3$ ) dissected at the indicated time points following injection.
- D, E Hematoxylin and eosin and immunohistological staining with A6, HNF4, Sox9 and CD133 antibodies of tumor sections from xenografts dissected 20 or 30 days after injection with primary hepatocytes from P240 *PR-SET7<sup>ΔHepA</sup>* livers.

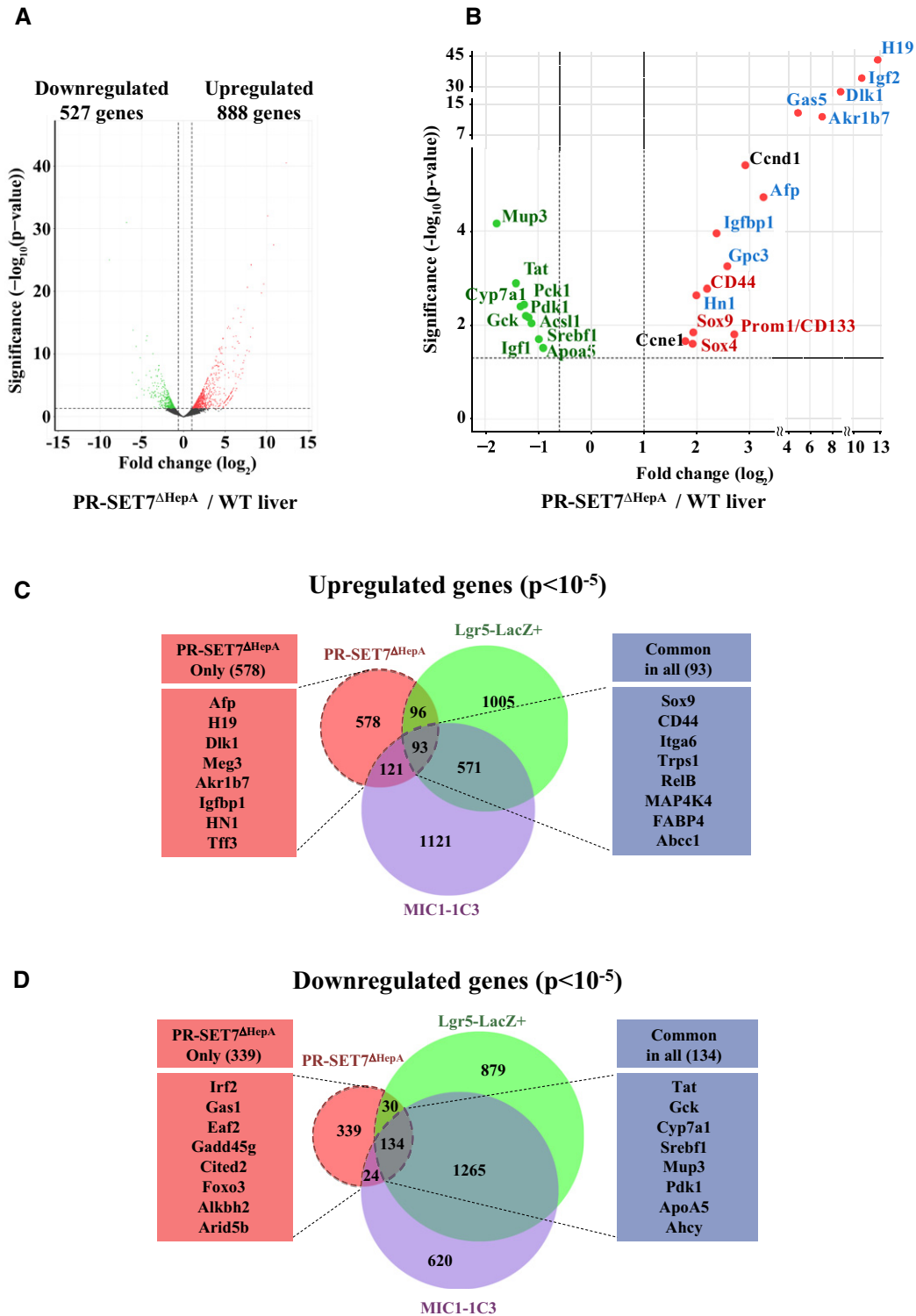


**Figure 8. Gene expression profile of P240 PR-SET7 $\Delta$ HepA livers and comparison with transcriptomes of ductal progenitor cells.**

- A Overexpression of stem cell-specific, oncofetal hepatic and proliferation-dependent genes in P240 PR-SET7 $\Delta$ HepA livers. Volcano plot of normalized RNAseq data obtained with P240 wild-type and PR-SET7 $\Delta$ HepA livers. Significance cutoff value was set at  $P = 0.05$  in  $-\log_{10}$  scale (horizontal dashed line) and fold change cutoffs at  $-0.6$  and  $1$  in  $\log_2$  scale (vertical dashed lines).
- B Volcano plots showing dots corresponding to representative stem cell marker genes (red), oncofetal hepatic genes (blue) and proliferation-dependent genes (black) are indicated.
- C, D Comparison of differentially expressed genes in P240 PR-SET7 $\Delta$ HepA livers with those reported in Lgr5-LacZ $^+$  sorted cells or MIC1-1C3 $^+$  sorted ductal cells (Huch et al, 2013).

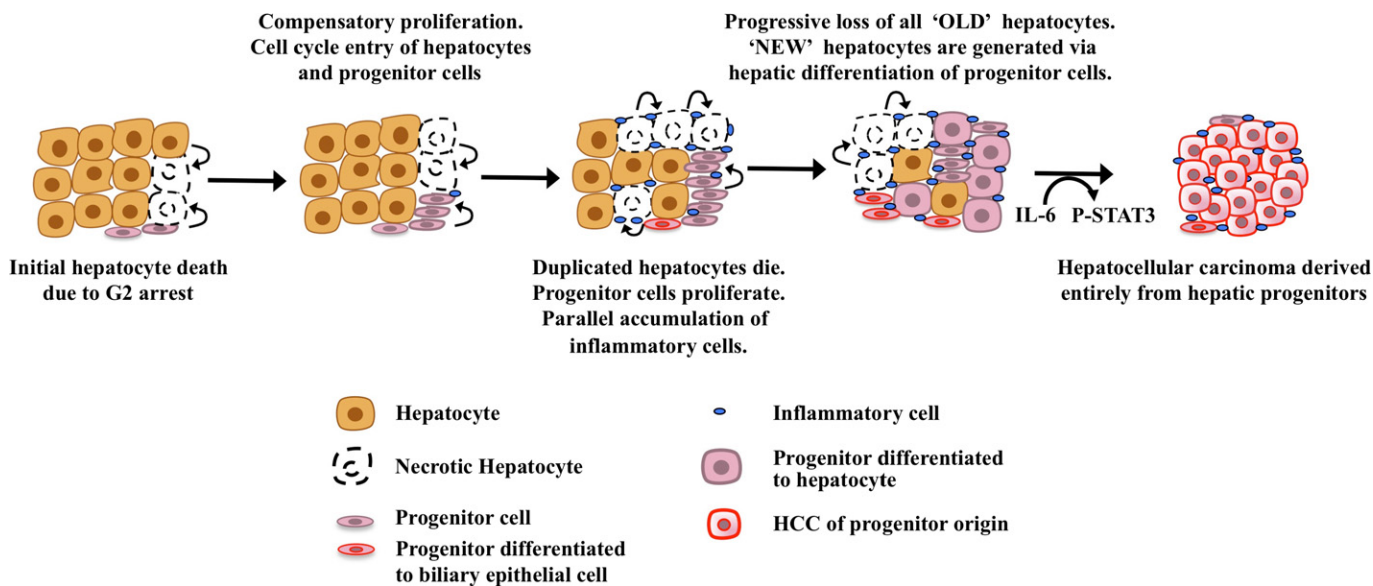


Figure 9. Schematic presentation of the temporal events leading to spontaneous hepatocellular carcinoma development in *PR-SET7*<sup>ΔHepA</sup> mice.

they display a cancer stem cell-specific gene expression signature featuring co-expression of ductal progenitor and hepatic oncofetal marker genes.

## Discussion

In this paper, we show that *PR-SET7* deficiency in fetal hepatocytes leads to necrosis and impairs liver organogenesis, while in postnatal liver it triggers regenerative processes that give rise to hepatocellular carcinoma. The resulting tumors are composed mainly of cells expressing ductal progenitor markers and possess functional features of cancer stem cells.

### *PR-SET7* deficiency in hepatocytes causes necrotic cell death

Previous studies have established the pivotal role of *PR-SET7* and H4K20 monomethylation in genome integrity. Loss of *PR-SET7* causes growth arrest due to enhanced DNA damage and defects in cell cycle progression (Jorgensen *et al*, 2007; Oda *et al*, 2009; Wu *et al*, 2010; Beck *et al*, 2012a,b). Standard *PR-SET7* knockout mouse embryos are not viable, as DNA damage-dependent growth arrest results in cell death prior to the embryonic eight-cell stage (Oda *et al*, 2009). Consistent with the above, we found that inactivation of *PR-SET7* in embryonic hepatoblasts results in genome instability, G2 phase arrest and massive cell death, which impairs proper liver organogenesis. The very fast loss of hepatocytes and the embryonic lethality in this animal model hampered more in-depth analysis of the cell death mechanism. Therefore, we inactivated *PR-SET7* in postnatal liver, which contains only few dividing hepatocytes, as the majority are in the resting G0 phase. The lack of phenotype at P45 (twenty days following the complete loss of *PR-SET7*) suggested that non-proliferating hepatocytes are relatively insensitive to *PR-SET7* inactivation, probably because H4K20 monomethylation is a stable histone modification that is erased mainly

through cell duplication. The requirement of cell division for H4K20Me<sub>1</sub> reduction and subsequent cell cycle arrest and death was demonstrated by the phenotype at later time points and by partial hepatectomy experiments, when G0-phase hepatocytes synchronously enter the cell cycle. In this latter experimental setup, all hepatocytes in *PR-SET7*<sup>ΔHepA</sup> mice were necrotic within 2 weeks after surgery.

Necrosis was the main mechanism of cell death in *PR-SET7*-deficient hepatocytes as evidenced by the classical necrosis-specific alterations.

### Mechanism of hepatocellular carcinoma development in *PR-SET7*-deficient mice

The main events that take place during postnatal development of *PR-SET7*<sup>ΔHepA</sup> mice are schematically presented in Fig 9. According to the model, initial death of a few hepatocytes in the postnatal liver triggers a local regenerative process whereby neighboring hepatocytes enter the cell cycle. Since all of the hepatocytes are deficient in *PR-SET7*, each of them is destined to undergo G2 phase arrest and necrotic cell death. In this way, compensatory proliferation, owing to the astonishing regenerative capacity of the liver, accelerates the death of the existing ('old') hepatocytes, which is expected to result in the complete elimination of all hepatocytes from the organ. This is avoided, however, by the parallel activation, proliferation and differentiation of Sox9<sup>+</sup> and A6<sup>+</sup> ductal progenitor cells, which will replenish the organ with 'new' hepatocytes. Progenitor cell activation is supported by a microenvironment producing an FGF7 signal. The activation of ductal progenitors in *PR-SET7*<sup>ΔHepA</sup> livers was clearly observable from postnatal day 120, when substantial numbers of hepatocytes had already undergone necrotic death. At this stage, most of the activated progenitors were HNF4 or albumin negative, suggesting that they have not yet differentiated into hepatocytes. Differentiation takes place at later stages, parallel to oncogenic transformation.

Deregulated expression of PR-SET7 in human HCCs has been reported previously (Takawa *et al*, 2012). In human liver cancers and other mouse hepatocellular carcinoma models, hepatocyte death initiates inflammation and fibrosis, which, when sustained for prolonged periods of time, invariably lead to compensatory proliferation-mediated hepatocarcinogenesis (Maeda *et al*, 2005; Luedde *et al*, 2007; Bettermann *et al*, 2010; He & Karin, 2011; Luedde & Schwabe, 2011; Nikolaou *et al*, 2012, 2013). Both of these pathologies develop spontaneously in the *PR-SET7<sup>AHepA</sup>* mice as early as 120 days of age and are sustained for at least 4 additional months, when full-blown liver cancer is detected. Prolonged inflammation and cell death result in the elevated production of IL-6 and parallel accumulation of reactive oxygen species (ROS). These trigger STAT3 activation, which leads to the oncogenic transformation of the newly generated hepatocytes (Fig 9). While the above pathologies closely mimic the major hallmarks of human HCC, hepatocellular carcinoma developing in the *PR-SET7<sup>AHepA</sup>* mice has a unique characteristic: It is composed exclusively of hepatic cancer stem cells (see below).

#### Cancer stem cell properties of hepatocellular carcinoma in PR-SET7-deficient mice

The existence of resident progenitor cells in the biliary ducts of the liver has recently been demonstrated using novel oval cell markers (Dorrell *et al*, 2011), FoxL1, Sox9 and Lgr5 (Sackett *et al*, 2009; Furuyama *et al*, 2011; Shin *et al*, 2011; Huch *et al*, 2013). These cells represent subpopulations of the well-known oval cells, identified by staining with the antibody A6 (Engelhardt *et al*, 1993). They reside in the biliary ductal epithelium and can be activated by various liver injuries, such as CCl<sub>4</sub>-treatment, DDC-diet or bile duct ligation. Importantly, they all have the potential to differentiate to either the hepatocyte or biliary epithelial cell lineage (Miyajima *et al*, 2014). Markers characterizing ductal progenitors (e.g. Sox9, CD133, EpCAM) are frequently used to identify 'cancer stem cells' (CSCs) in hepatocellular carcinoma (Ma *et al*, 2010; Marquardt *et al*, 2011; Zhao *et al*, 2013). Cancer stem cells are operationally defined as the subset (1–6% in human HCC) of cells with stem cell properties, capable of self-renewal and of giving rise to the heterogeneous population of neoplastic cells organized hierarchically in the tumors (Ma *et al*, 2007; Yang *et al*, 2008; Magee *et al*, 2012).

The origin of hepatic CSCs is unclear. In principle, the expression of progenitor markers in hepatic CSCs implies that they represent either an expanded population of transformed proliferating ductal progenitor cells acquiring hepatocyte-like features or a population of transformed hepatocytes displaying progenitor-like properties. In the first case, transformed progenitors may arise via differentiation and oncogenic transformation of the normal progenitor cells, while in the second case stem cell properties can be acquired via 'de-differentiation' of hepatocytes. Pertinent to this, recent lineage tracing studies have demonstrated that hepatocytes can also undergo widespread reprogramming to the biliary epithelial cell lineage or to cells bearing progenitor properties, following liver damage, intrahepatic cholangiocarcinoma formation or inactivation of the Hippo signaling pathway (Fan *et al*, 2012; Sekiya & Suzuki, 2012; Yanger *et al*, 2013; Yimlamai *et al*, 2014). This raises the idea that partial reprogramming of cancerous hepatocytes to cells with

ductal progenitor properties may take place in tumors developing under specific injury conditions.

Support to the 'de-differentiation' hypothesis was provided by the recent identification of *bona fide* HCC progenitor cells (HcPCs) in injury-induced mouse HCC models (He *et al*, 2013). These cells have tumor initiation properties when transplanted to livers undergoing chronic damage and acquire autocrine IL-6 signaling that stimulates their malignant progression. Relevant to the current study, the gene expression profile of HcPCs shows high levels of similarity to the ductal progenitor cell population specified by FoxL1 expression (Shin *et al*, 2011). However, the generation of HcPCs depends on DEN-mediated liver damage, a drug that can act only on differentiated hepatocytes expressing high levels of Cyp2E1 (Kang *et al*, 2007). This implies that HcPCs most likely originate from mature hepatocytes and subsequently undergo a damage-induced de-differentiation process (He *et al*, 2013). P240 *PR-SET7<sup>AHepA</sup>* hepatocytes and HcPCs correspond to different cell populations. This notion is supported by their different gene expression patterns and by key differences in their tumorigenic properties: Unlike P240 *PR-SET7<sup>AHepA</sup>* hepatocytes, HcPCs cannot form subcutaneous tumors or even liver tumors when introduced to non-damaged livers (He *et al*, 2013). They can give rise to cancer only when transplanted to livers under chronic damage and compensatory proliferation.

Our results may be more compatible with an alternative to the above de-differentiation concept, raising the possibility that cancer stem cells may originate from normally existing progenitor cell populations. The key evidence for the notion that HCC in *PR-SET7<sup>AHepA</sup>* mice may arise via the oncogenic transformation of an expanded population of differentiating ductal progenitors, rather than via de-differentiation of transformed hepatocytes, is that PR-SET7-deficient hepatocytes are destined to death by necrosis once they enter the cell cycle. Thus, they cannot provide a source of highly proliferating cancerous cells that would subsequently de-differentiate to CSCs.

On the other hand, since direct lineage tracing experiments cannot be performed in the Cre-lox system-mediated PR-SET7 KO model, the possibility that some hepatocytes escape Cre-mediated recombination and due to the strong selective pressure de-differentiate and repopulate the liver cannot be entirely excluded. This possibility is also supported by recent studies demonstrating that existing hepatocytes and not progenitors generate new hepatocytes in different injury-mediated liver regeneration models (Schaub *et al*, 2014; Yanger *et al*, 2014). In contrast, several findings presented in this study are not compatible with an 'escaper' hypothesis. For example, at early time points of the process, Sox9/HNF4 or A6/HNF4 double-positive hepatocytes cannot be detected in PR-SET7-deficient livers. If de-differentiating 'escapers' of Cre-recombination played a role, they should have expanded substantially and easily be detected at least at P120, when massive cell death was already widespread. Instead, we observed solely the expansion of undifferentiated progenitor cells (A6<sup>+</sup>/HNF4<sup>-</sup> and Sox9<sup>+</sup>/Alb<sup>-</sup>), which preceded the activation of oncogenic STAT3 and the first appearance of cells expressing both progenitor and hepatic markers. This time course of events is only compatible with a partial differentiation of ductal progenitors toward hepatocytes and not the other way around. Secondly, such potential 'escaper' hepatocytes should have been capable of regenerating the liver within 1 week after partial hepatectomy. Instead, we observed only necrotic hepatocytes in the

*PR-SET7<sup>AHepA</sup>* livers 2 weeks after the surgery and an early (after 1–2 months) lethality of the mice. Furthermore, when compensatory growth of remnant hepatocytes gives rise to HCC in a similar setting of liver damage and inflammation (e.g. in DEN-induced hepatocarcinogenesis), the number of hepatocytes expressing A6 or Sox9 is in the range of 2–5%, as opposed to 97% observed in P240 *PR-SET7<sup>AHepA</sup>* livers. In agreement with this, we identified a large number of genes whose expression was differentially changed in P240 *PR-SET7<sup>AHepA</sup>* livers compared to DEN-induced tumors. Finally, the very low similarity between the differentially expressed genes of P240 *PR-SET7<sup>AHepA</sup>* livers and the hepatocyte-derived, de-differentiated HcPCs also argues against the potential involvement of de-differentiating ‘escapers’ in the observed phenotype. We note, however, that although the above arguments indirectly support the progenitor origin of hepatocytes in P240 *PR-SET7<sup>AHepA</sup>* livers, they do not provide unequivocal evidence to rule out ‘escaper’ hepatocyte origin.

P240 *PR-SET7<sup>AHepA</sup>* hepatocytes express several markers, such as Sox9, CD133, EpCAM, CD44, which are used to identify CSCs, and oncofetal marker genes, which are used to identify HCC. These features suggest that P240 *PR-SET7<sup>AHepA</sup>* hepatocytes resemble transformed immature cancer cell characteristic of highly aggressive tumors. Their potential to self-renew in culture and give rise to tumors containing stem cell marker-expressing cells and more differentiated cells in xenografts demonstrates that they correspond to cancer stem cells. If, as speculated above, these CSCs originate from ductal progenitors, they probably retain stem cell properties of their ancestors throughout the differentiation and oncogenic transformation process.

#### Hepatic cancer stem cell transcriptome specified by the coexpression of ductal progenitor and hepatic oncofetal genes

Ductal progenitors in mouse livers represent a mixed population of cells (Dorrell *et al*, 2011; Shin *et al*, 2011; Huch *et al*, 2013), which was confirmed by double staining for Sox9 and A6 (Supplementary Fig S5F) and comparisons of gene expression patterns (Supplementary Fig S6B–D). The CSCs in the *PR-SET7<sup>AHepA</sup>* mice also display a mixed phenotype, expressing different combinations of progenitor markers. Differentially expressed genes (relative to wild-type livers) in the cancerous *PR-SET7<sup>AHepA</sup>* livers overlap significantly with those identified in different normal ductal cell populations (*Lgr5-LacZ<sup>+</sup>* and *MIC1C3<sup>+</sup>*), pointing to a close biological relationship between them. Our comparisons of differentially expressed genes established a specific hepatic cancer stem cell gene signature with the following features: (A) high expression of ductal progenitor markers; (B) high expression of hepatic oncofetal genes; (C) high expression of proliferation-specific genes; (D) decreased expression of tumor suppressor genes; (E) downregulation of genes expressed specifically in terminally differentiated hepatocytes. As expected, most of the overlap between the differentially expressed gene set in *PR-SET7<sup>AHepA</sup>* livers and normal ductal progenitors was detected in gene categories A and E.

Collectively our results suggest that hepatocellular carcinoma in *PR-SET7<sup>AHepA</sup>* mice has a cancer stem cell phenotype combining fetal hepatoblast-like and ductal progenitor cell-like features. These animals therefore represent a useful model for studying and testing drugs targeting hepatic cancer stem cells.

## Materials and Methods

### Animals

The generation of *PR-SET7<sup>loxP</sup>* mice carrying floxed exon 7 allele of *PR-SET7* has been described previously (Oda *et al*, 2009). These mice were maintained in mixed C57Bl6/CBA background and crossed with either *Alfp-Cre* or *Alb-Cre* mice (Yakar *et al*, 1999; Kellendonk *et al*, 2000; Kymizi *et al*, 2006) to obtain hepatocyte-specific inactivation of the *PR-SET7* gene in embryonic and adult liver, respectively. In the mixed C57Bl6/CBA background, *Alb-Cre* mice expressed detectable amounts of the transgene only after birth. Mice were maintained in grouped cages in a temperature-controlled, pathogen-free facility on a 12-h light/dark cycle and fed by a standard chow diet (Altromin 1324; 19% protein, 5% fat) and water *ad libitum*. 2/3<sup>rd</sup> partial hepatectomy was performed in anaesthetized animals by resecting the median and left lobes. Control mice were sham operated. All animal experiments were approved by the Prefecture of Attica and were performed in accordance with the respective national and European Union regulations. All the experiments were performed in randomly chosen age-matched male mice. Typically, each experiment was performed in materials from at least three individual mice. No blinding was used in this study.

### Histological analysis

Hematoxylin and eosin, Sirius Red, TUNEL staining and immunohistochemistry with fluorescent secondary antibodies in formalin-fixed paraffin-embedded or frozen sections were performed as described previously (Nikolaou *et al*, 2012). Immunohistochemical assays via detection of oxidized 3,3'-diaminobenzidine (DAB) substrate were performed by using the Signalstain DAB Substrate kit (Cell Signaling Technology). Briefly, frozen sections were fixed with 4% formaldehyde, blocked with 1% BSA and 0.1% Triton X-100 and incubated with the primary antibodies overnight at 4°C. After washing, the sections were incubated with DAB solution and counterstained with hematoxylin. The antibodies used for the stainings are described in the Supplementary Materials and Methods.

For electron microscopy, liver tissues were fixed for 2 h at room temperature in 0.08 M sodium cacodylate buffer, containing 2% of each glutaraldehyde and paraformaldehyde, followed by 1 h postfixation with 1% osmium tetroxide. Upon 1% uranyl acetate treatment for 20 min, samples were dehydrated with ethanol series and subsequently embedded in LR White resin/propylene oxide (Polysciences). Approximately 100 nm thin sections on copper grids were observed at 80 kV with a JEOL JM2100 transmission electron microscope.

### Antibodies

The antibodies used in this study were from the following: Santa Cruz Biotechnology: anti-HNF4 (sc-8987), anti-AFP (sc-8108), anti-Pr-Set7 (sc-135009), anti-53BP1 (sc-22760) and anti-FGF7 (SC-27127); Cell Signaling Technology: anti-cyclin B1 (#4138), anti-Stat3 (#9132), anti-phospho-Stat3 (#9145) and anti-phospho-histone H2A.X (#9718); Abcam: anti-Ki67 (ab15580), anti-histone H4 mono

methyl K20 (ab9051), anti-histone H4 tri methyl K20 (ab9053) and anti-Pr-Set7 (ab3798); Bethyl Laboratories, anti-Alb (A90–234); AbD Serotec, anti-F4/80 (MCA497); Merck-Millipore, anti-Sox9 (AB5535) and anti-Prominin-CD133 (MAB4310); Biolegend, anti-CD45 (#103101); and DAKO, anti-CK19 (#A0575). The A6 antibody was obtained from Valentina Factor (NIH).

### Biochemical analysis

Liver extracts were prepared by homogenizing liver tissues in 20 volume of a buffer containing 50 mM Tris pH 7.5, 1% NP-40, 0.25% sodium deoxycholate, 150 mM NaCl, 1 mM EDTA, 10% glycerol and protease inhibitor cocktail (Roche) using polytron tissue homogenizer at 20,000 stroke setting. After centrifugation, the cleared lysates were subjected to SDS-PAGE and Western blot analysis as described in Tatarakis *et al* (2008) and Kontaki and Talianidis (2010). Alanine aminotransferase (ALT) activity was measured in freshly isolated plasma fractions using the ALT assay kit from Dysis.

### RNA analysis

Total RNA was prepared by TRIzol extraction followed by digestion with DNase I. Reverse transcription and quantitative real-time PCR assays were performed as described previously (Tatarakis *et al*, 2008). The statistical significance of the data was evaluated by Student's *t*-test. The nucleotide sequences of the primer sets are described in the Supplementary Materials and Methods.

RNA-seq was performed on an Ion Proton™ System (Rothberg *et al*, 2011), according to the manufacturer's instructions. Briefly, approximately 20 µg of total RNAs was used for mRNA isolation using the Dynabeads mRNA DIRECT™ Micro Kit (Life Technologies, Carlsbad, CA, USA). The isolated mRNA was digested with RNase III, hybridized and ligated to Ion Adaptors, reverse transcribed, barcoded and amplified, using the Ion Total RNA-Seq Kit v2 (Life Technologies). Samples were processed on an OneTouch 2 instrument and enriched on a One Touch ES station. Templating was performed using the Ion PI™ Template OT2 200 Kit (Life Technologies) and sequencing with the Ion PI™ Sequencing 200 Kit on Ion Proton PI™ chips (Life Technologies) according to commercially available protocols. Methods used for the analyses of the RNAseq data are described in the Supplementary Materials and Methods.

### Xenograft experiments

Primary hepatocytes were isolated from P240 *PR-SET7<sup>AHepA</sup>* mice using collagenase perfusion protocol (Tatarakis *et al*, 2008). The cells were seeded to tissue culture plates coated with 50 µg/ml rat collagen (type 1) and cultured in a medium containing DMEM/F12, 10% fetal bovine serum (FBS), 5 µg/ml insulin, 5 µg/ml transferin, 5 ng/ml selenious acid, 10<sup>-7</sup> M dexamethasone and 20 ng/ml EGF. The cells could survive at least four passages in the same culture conditions without significant loss of growth rate. About 10<sup>6</sup> cultured primary cells were mixed with BD-Matrigel matrix in 1:1 ration and injected into the right flank of two-month-old *Rag1<sup>-/-</sup>* mice. As a control, the same number of Hepa 1–6 cells (ATCC) was

used for injection. Subcutaneous tumors were isolated, and their volume was measured at various times after the initial injection.

### Accession Numbers

Gene expression data and CGH data were deposited in Gene Expression Omnibus (GEO) under accession numbers GSE49555 and GSE61567, respectively.

**Supplementary information** for this article is available online:

<http://emboj.embopress.org>

### Acknowledgements

We thank V. Harokopos and K. Lilakos for assistance in RNAseq experiments and Dr S. Kotschote (IMGM Laboratories) for performing CGH hybridizations. This work was supported by the ERC Advanced Investigator Grant (ERC-2011-AdG294464) and the EU program NR-NET (PITN-GA-2013-606806).

### Author contributions

KCN conceived, designed and performed experiments and analyzed the data. PM performed the bioinformatics analysis. GC and PH performed experiments and analyzed the data. HO and DR provided floxed PR-SET7 mice. IT conceived the project, designed experiments, analyzed the data and wrote the manuscript.

### Conflict of interest

The authors declare that they have no conflict of interest.

## References

- Abbas T, Shibata E, Park J, Jha S, Karnani N, Dutta A (2010) CRL4(Cdt2) regulates cell proliferation and histone gene expression by targeting PR-Set7/Set8 for degradation. *Mol Cell* 40: 9–21
- Beck DB, Burton A, Oda H, Ziegler-Birling C, Torres-Padilla ME, Reinberg D (2012a) The role of PR-Set7 in replication licensing depends on Suv4-20h. *Genes Dev* 26: 2580–2589
- Beck DB, Oda H, Shen SS, Reinberg D (2012b) PR-Set7 and H4K20me1: at the crossroads of genome integrity, cell cycle, chromosome condensation, and transcription. *Genes Dev* 26: 325–337
- Bettermann K, Vucur M, Haybaeck J, Koppe C, Janssen J, Heymann F, Weber A, Weiskirchen R, Liedtke C, Gassler N, Müller M, de Vos R, Wolf MJ, Boege Y, Seleznik GM, Zeller N, Erny D, Fuchs T, Zoller S, Cairo S, Buendia MA, Prinz M, Akira S, Tacke F, Heikenwalder M, Trautwein C, Luedde T (2010) TAK1 suppresses a NEMO-dependent but NF-κB-independent pathway to liver cancer. *Cancer Cell* 17: 481–496
- Centore RC, Havens CG, Manning AL, Li JM, Flynn RL, Tse A, Jin J, Dyson NJ, Walter JC, Zou L (2010) CRL4(Cdt2)-mediated destruction of the histone methyltransferase Set8 prevents premature chromatin compaction in S phase. *Mol Cell* 40: 22–33
- Chaffer CL, Marjanovic ND, Lee T, Bell G, Kleer CG, Reinhardt F, D'Alessio AC, Young RA, Weinberg RA (2013) Poised chromatin at the ZEB1 promoter enables breast cancer cell plasticity and enhances tumorigenicity. *Cell* 154: 61–74
- Dorrell C, Erker L, Schug J, Kopp JL, Canaday PS, Fox AJ, Smirnova O, Duncan AW, Finegold MJ, Sander M *et al* (2011) Prospective isolation of a bipotential clonogenic liver progenitor cell in adult mice. *Genes Dev* 25: 1193–1203

- Engelhardt NV, Factor VM, Medvinsky AL, Baranov VN, Lazareva MN, Poltoranina VS (1993) Common antigen of oval and biliary epithelial cells (A6) is a differentiation marker of epithelial and erythroid cell lineages in early development of the mouse. *Differentiation* 55: 19–26
- Español-Suñer R, Carpentier R, Van Hul N, Legry V, Achouri Y, Cordi S, Jacquemin P, Lemaigre F, Leclercq IA (2012) Liver progenitor cells yield functional hepatocytes in response to chronic liver injury in mice. *Gastroenterology* 143: 1564–1575
- Fan B, Malato Y, Calvisi DF, Naqvi S, Razumilava N, Ribback S, Gores GJ, Dombrowski F, Evert M, Chen X, Willenbring H (2012) Cholangiocarcinomas can originate from hepatocytes in mice. *J Clin Invest* 122: 2911–2915
- Friedman JR, Kaestner KH (2011) On the origin of the liver. *J Clin Invest* 121: 4630–4633
- Friedmann-Morvinski D, Bushong EA, Ke E, Soda Y, Marumoto T, Singer O, Ellisman MH, Verma IM (2012) Dedifferentiation of neurons and astrocytes by oncogenes can induce gliomas in mice. *Science* 338: 1080–1084
- Furuyama K, Kawaguchi Y, Akiyama H, Horiguchi M, Kodama S, Kuhara T, Hosokawa S, Elbahrawy A, Soeda T, Koizumi M et al (2011) Continuous cell supply from a Sox9-expressing progenitor zone in adult liver, exocrine pancreas and intestine. *Nat Genet* 43: 34–41
- He G, Dhar D, Nakagawa H, Font-Burgada J, Ogata H, Jiang Y, Shalpour S, Seki E, Yost SE, Jepsen K, Frazer KA, Harismendy O, Hatziaepostolou M, Iliopoulos D, Suetsugu A, Hoffman RM, Tateishi R, Koike K, Karin M (2013) Identification of liver cancer progenitors whose malignant progression depends on autocrine IL-6 signaling. *Cell* 155: 384–396
- He G, Karin M (2011) NF- $\kappa$ B and STAT3—key players in liver inflammation and cancer. *Cell Res* 21: 159–168
- Huch M, Dorrell C, Boj SF, van Es JH, Li VS, van de Wetering M, Sato T, Hamer K, Sasaki N, Finegold MJ et al (2013) In vitro expansion of single Lgr5<sup>+</sup> liver stem cells induced by Wnt-driven regeneration. *Nature* 494: 247–250
- Jorgensen S, Elvers I, Trelle MB, Menzel T, Eskildsen M, Jensen ON, Helleday T, Helin K, Sorensen CS (2007) The histone methyltransferase SET8 is required for S-phase progression. *J Cell Biol* 179: 1337–1345
- Kang JS, Wanibuchi H, Morimura K, Gonzalez FJ, Fukushima S (2007) Role of CYP2E1 in diethylnitrosamine-induced hepatocarcinogenesis in vivo. *Cancer Res* 67: 11141–11146
- Kellendonk C, Opherck C, Anlag K, Schutz G, Tronche F (2000) Hepatocyte-specific expression of Cre recombinase. *Genesis* 26: 151–153
- Kontaki H, Talianidis I (2010) Lysine methylation regulates E2F1-induced cell death. *Mol Cell* 39: 152–160
- Kyrmizi I, Hatzis P, Katrakili N, Tronche F, Gonzalez FJ, Talianidis I (2006) Plasticity and expanding complexity of the hepatic transcription factor network during liver development. *Genes Dev* 20: 2293–2305
- Luedde T, Beraza N, Kotsikoris V, van Loo G, Nenci A, De Vos R, Roskams T, Trautwein C, Pasparakis M (2007) Deletion of NEMO/IKK $\gamma$  in liver parenchymal cells causes steatohepatitis and hepatocellular carcinoma. *Cancer Cell* 11: 119–132
- Luedde T, Schwabe RF (2011) NF- $\kappa$ B in the liver—linking injury, fibrosis and hepatocellular carcinoma. *Nat Rev Gastroenterol Hepatol* 8: 108–118
- Ma S, Chan KW, Hu L, Lee TK, Wo JY, Ng IO, Zheng BJ, Guan XY (2007) Identification and characterization of tumorigenic liver cancer stem/progenitor cells. *Gastroenterology* 132: 2542–2556
- Ma S, Tang KH, Chan YP, Lee TK, Kwan PS, Castilho A, Ng I, Man K, Wong N, To KF et al (2010) miR-130b Promotes CD133(+) liver tumor-initiating cell growth and self-renewal via tumor protein 53-induced nuclear protein 1. *Cell Stem Cell* 7: 694–707
- Maeda S, Kamata H, Luo JL, Leffert H, Karin M (2005) IKK $\beta$  couples hepatocyte death to cytokine-driven compensatory proliferation that promotes chemical hepatocarcinogenesis. *Cell* 121: 977–990
- Magee JA, Piskounova E, Morrison SJ (2012) Cancer stem cells: impact, heterogeneity, and uncertainty. *Cancer Cell* 21: 283–296
- Majumdar A, Curley SA, Wu X, Brown P, Hwang JP, Shetty K, Yao ZX, He AR, Li S, Katz L et al (2012) Hepatic stem cells and transforming growth factor  $\beta$  in hepatocellular carcinoma. *Nat Rev Gastroenterol Hepatol* 9: 530–538
- Malato Y, Naqvi S, Schurmann N, Ng R, Wang B, Zape J, Kay MA, Grimm D, Willenbring H (2011) Fate tracing of mature hepatocytes in mouse liver homeostasis and regeneration. *J Clin Invest* 121: 4850–4860
- Marquardt JU, Raggi C, Andersen JB, Seo D, Avital I, Geller D, Lee YH, Kitade M, Holczbauer A, Gillen MC et al (2011) Human hepatic cancer stem cells are characterized by common stemness traits and diverse oncogenic pathways. *Hepatology* 54: 1031–1042
- Medema JP (2013) Cancer stem cells: the challenges ahead. *Nat Cell Biol* 15: 338–344
- Miyajima A, Tanaka M, Itoh T (2014) Stem/progenitor cells in liver development, homeostasis, regeneration, and reprogramming. *Cell Stem Cell* 14: 561–574
- Nikolaou K, Sarris M, Talianidis I (2013) Molecular pathways: the complex roles of inflammation pathways in the development and treatment of liver cancer. *Clin Cancer Res* 19: 2810–2816
- Nikolaou K, Tsgaratou A, Eftychi C, Kollias G, Mosialos G, Talianidis I (2012) Inactivation of the deubiquitinase CYLD in hepatocytes causes apoptosis, inflammation, fibrosis, and cancer. *Cancer Cell* 21: 738–750
- Oda H, Hubner MR, Beck DB, Vermeulen M, Hurwitz J, Spector DL, Reinberg D (2010) Regulation of the histone H4 monomethylase PR-Set7 by CRL4 (Cdt2)-mediated PCNA-dependent degradation during DNA damage. *Mol Cell* 40: 364–376
- Oda H, Okamoto I, Murphy N, Chu J, Price SM, Shen MM, Torres-Padilla ME, Heard E, Reinberg D (2009) Monomethylation of histone H4-lysine 20 is involved in chromosome structure and stability and is essential for mouse development. *Mol Cell Biol* 29: 2278–2295
- Rothberg JM, Hinz W, Rearick TM, Schultz J, Mileski W, Davey M, Leamon JH, Johnson K, Milgrew MJ, Edwards M et al (2011) An integrated semiconductor device enabling non-optical genome sequencing. *Nature* 475: 348–352
- Sackett SD, Li Z, Hurtt R, Gao Y, Wells RG, Brondell K, Kaestner KH, Greenbaum LE (2009) Foxl1 is a marker of bipotential hepatic progenitor cells in mice. *Hepatology* 49: 920–929
- Schaub JR, Malato Y, Gormond C, Willenbring H (2014) Evidence against a stem cell origin of new hepatocytes in a common mouse model of chronic liver injury. *Cell Rep* 8: 933–939
- Schwitala S, Fingerle AA, Cammareri P, Nebelsiek T, Goktuna SI, Ziegler PK, Canli O, Heijmans J, Huels DJ, Moreaux G et al (2013) Intestinal tumorigenesis initiated by dedifferentiation and acquisition of stem-cell-like properties. *Cell* 152: 25–38
- Sekiya S, Suzuki A (2012) Intrahepatic cholangiocarcinoma can arise from Notch-mediated conversion of hepatocytes. *J Clin Invest* 122: 3914–3918
- Shin S, Walton G, Aoki R, Brondell K, Schug J, Fox A, Smirnova O, Dorrell C, Erker L, Chu AS et al (2011) Foxl1-Cre-marked adult hepatic progenitors have clonogenic and bilineage differentiation potential. *Genes Dev* 25: 1185–1192
- Takase HM, Itoh T, Ino S, Wang T, Koji T, Akira S, Takikawa Y, Miyajima A (2013) FGF7 is a functional niche signal required for stimulation of adult

- liver progenitor cells that support liver regeneration. *Genes Dev* 27: 169–181
- Takawa M, Cho HS, Hayami S, Toyokawa G, Kogure M, Yamane Y, Iwai Y, Maejima K, Ueda K, Masuda A et al (2012) Histone lysine methyltransferase SETD8 promotes carcinogenesis by deregulating PCNA expression. *Cancer Res* 72: 3217–3227
- Tatarakis A, Margaritis T, Martinez-Jimenez CP, Kouskouti A, Mohan WS 2nd, Haroniti A, Kafetzopoulos D, Tora L, Talianidis I (2008) Dominant and redundant functions of TFIID involved in the regulation of hepatic genes. *Mol Cell* 31: 531–543
- Wang EY, Yeh SH, Tsai TF, Huang HP, Jeng YM, Lin WH, Chen WC, Yeh KH, Chen PJ, Chen DS (2011) Depletion of  $\beta$ -catenin from mature hepatocytes of mice promotes expansion of hepatic progenitor cells and tumor development. *Proc Natl Acad Sci USA* 108: 18384–918389
- Wu S, Wang W, Kong X, Congdon LM, Yokomori K, Kirschner MW, Rice JC (2010) Dynamic regulation of the PR-Set7 histone methyltransferase is required for normal cell cycle progression. *Genes Dev* 24: 2531–2542
- Yakar S, Liu JL, Stannard B, Butler A, Accili D, Sauer B, LeRoith D (1999) Normal growth and development in the absence of hepatic insulin-like growth factor I. *Proc Natl Acad Sci USA* 96: 7324–7329
- Yamaji S, Zhang M, Zhang J, Endo Y, Bibikova E, Goff SP, Cang Y (2010) Hepatocyte-specific deletion of DDB1 induces liver regeneration and tumorigenesis. *Proc Natl Acad Sci USA* 107: 22237–22242
- Yang ZF, Ho DW, Ng MN, Lau CK, Yu WC, Ngai P, Chu PW, Lam CT, Poon RT, Fan ST (2008) Significance of CD90<sup>+</sup> cancer stem cells in human liver cancer. *Cancer Cell* 13: 153–166
- Yanger K, Knigin D, Zong Y, Maggs L, Gu G, Akiyama H, Pikarsky E, Stanger BZ (2014) Adult hepatocytes are generated by self-duplication rather than stem cell differentiation. *Cell Stem Cell* 15: 340–349
- Yanger K, Zong Y, Maggs LR, Shapira SN, Maddipati R, Aiello NM, Thung SN, Wells RG, Greenbaum LE, Stanger BZ (2013) Robust cellular reprogramming occurs spontaneously during liver regeneration. *Genes Dev* 27: 719–724
- Yimlamai D, Christodoulou C, Galli GG, Yanger K, Pepe-Mooney B, Gurung B, Shrestha K, Cahan P, Stanger BZ, Camargo FD (2014) Hippo pathway activity influences liver cell fate. *Cell* 157: 1324–1338
- Zhao W, Wang L, Han H, Jin K, Lin N, Guo T, Chen Y, Cheng H, Lu F, Fang W et al (2013) 1B50-1, a mAb raised against recurrent tumor cells, targets liver tumor-initiating cells by binding to the calcium channel  $\alpha$ 2delta1 subunit. *Cancer Cell* 23: 541–556



**License:** This is an open access article under the terms of the Creative Commons Attribution-NonCommercial-NoDerivs 4.0 License, which permits use and distribution in any medium, provided the original work is properly cited, the use is non-commercial and no modifications or adaptations are made.